Pramana – J. Phys. (2019) 93:60
https://doi.org/10.1007/s12043-019-1821-4

Nuclear multipole excitations in the framework of self-consistent Hartree–Fock random phase approximation for Skyrme forces

ALI H TAQI* and EBTIHAL G KHIDHER

Department of Physics, College of Science, Kirkuk University, Kirkuk, Iraq
*Corresponding author. E-mail: alitaqi@uokirkuk.edu.iq

MS received 14 January 2018; revised 2 March 2019; accepted 22 April 2019

Abstract. In this study, the fully self-consistent Hartree–Fock (HF)-based random phase approximation (RPA) calculations were done for the ^{40}Ca and ^{48}Ca nuclei using 20 Skyrme-type interactions: KDE0, KDE0v1, SLy4, SLy5, SLy6, SK255, SKI2, SKI3, SKI5, SKM, SKMP, SKP, LNS, SGII, RAPT, SV-bas, SV-m56-O, SV-m64-O, SV-min and T6. Having a large number of Skyrme-force parameterisations requires a continuous search for the best for describing the experimental data. To examine our results, we compared the strength functions $S(E)$, the charge density distribution and centroid energies E_{CEN} of the isoscalar giant monopole resonance (ISGMR), $J^{\pi} = 0^{+}$, $T = 0$, the isovector giant dipole resonance (IVGDR), $J^{\pi} = 1^{-}$, $T = 1$, and isoscalar giant quadrupole resonance (ISGQR), $J^{\pi} = 2^{+}$, $T = 0$ with the available experimental data. Moreover, we discussed the sensitivities of the centroid energy m_1/m_0 and moment m_1 of the $S(E)$ to the bulk properties of nuclear matter (NM), such as K_{NM}, the effective mass m^*/m and the enhancement factor κ.

Keywords. Nuclear structure; Skyrme–Hartree–Fock; collective excitations.

PACS Nos **21.45.−v; 21.10.−k; 21.60.Ev**

1. Introduction

The understanding of the properties and structure of nuclei has been unsatisfactory even after decades. So, to have a universal approach to describe the nuclei with accuracy was the aim of the experimental and theoretical studies. The problem of nuclear structure is a many-body problem, as it arises in many branches of physics. The dimension of Hilbert space rapidly grows as the particle number increases and the dimension of such space is too large in many cases, preventing us from performing full calculations. Therefore, various approximate methods have been used to deal with such systems.

The field has advanced in the past few decades because of the improvements in computer technology and availability of computational resources. On the theoretical front, computationally intensive *ab-initio* methods using the bare nucleon–nucleon (NN) interaction, and advanced methods such as Green's function Monte Carlo (GFMC) [1], no-core shell model (NCSM) [2], coupled cluster (CC) [3], self-consistent Green's function (SCGF) [4] and in-medium similarity renormalisation group (IM-SRG) [5] have been used with great success in light nuclei, typically with $A \precsim 15$. Things get more complex in heavier systems. One way out is to deal with these systems in a nuclear matter (NM) framework [6].

The NM equation of state (EOS) essentially describes the binding energy per nucleon as a function of neutron (N) and proton (Z) densities. For symmetric NM, the saturation point is well determined from the measured binding energies and central matter densities of the nuclei, by extrapolation to infinite NM [7,8]. Beyond the saturation point of the symmetric NM, an accurate value of the NM incompressibility coefficient K_{NM}, which is directly related to the curvature of the EOS of the symmetric NM, is needed. An accurate knowledge of the dependence of the symmetry energy, $E_{\mathrm{sym}}(\rho)$, on the matter density ρ is needed for the EOS of asymmetric NM. There have been many attempts over the years to determine K_{NM} and $E_{\mathrm{sym}}(\rho)$ by considering physical quantities which are sensitive to the values of K_{NM} and $E_{\mathrm{sym}}(\rho)$ [9–12]. Others investigated the sensitivity of the strength function distributions $S(E)$ to K_{NM}, $E_{\mathrm{sym}}(\rho)$ and the effective mass m^*/m [13,14].

Published online: 17 July 2019

Table 1. Values of the parameters for the following Skyrme interaction.

Force	t_0	t_1	t_2	t_3	W_0	x_0	x_1	x_2	x_3	X_w	α
KDE0	−2526.51	430.94	−398.38	14235.52	128.96	0.7583	−0.3087	−0.9495	1.1445	1.0000	0.167
KDE0v1	−2553.08	411.70	−419.87	14603.61	124.41	0.6483	−0.3472	−0.9268	0.9475	1.0000	0.167
SLy4	−2488.91	486.82	−546.39	13777.00	123.00	0.8340	−0.3440	−1.0000	1.3540	1.0000	0.167
SLy5	−2484.88	483.13	−549.40	13763.00	126.00	0.7780	−0.3280	−1.0000	1.2670	1.0000	0.167
SLy6	−2479.50	462.18	−448.61	13673.00	122.00	0.8250	−0.4650	−1.0000	1.3550	1.0000	0.167
SK255	−1689.35	389.30	−126.07	10989.60	95.39	−0.1461	0.1660	0.0012	−0.7449	1.0000	0.356
SKI2	−1915.43	438.449	305.446	10548.9	120.60	−0.2108	−1.737	−1.5336	−0.178	1.0000	0.250
SKI3	−1762.88	561.61	−227.09	8106.20	188.51	0.3083	−1.1722	−1.0907	1.2926	0.0000	0.250
SKI5	−1772.91	550.84	−126.69	8206.25	123.63	−0.1171	−1.3088	−1.0487	0.3410	1.0000	0.250
SKM	−2645.00	410.00	−135.00	15595.00	130.00	0.0900	0.0000	0.0000	0.0000	1.0000	0.167
SKMP	−2372.24	503.62	57.28	12585.30	160.00	−0.1576	−0.4029	−2.9557	−0.2679	1.0000	0.167
SKP	−2931.70	320.62	−337.41	18708.97	100.00	0.2922	0.6532	−0.5373	0.1810	1.0000	0.167
LNS	−2484.97	266.74	−337.14	14588.20	96.00	0.0628	0.6585	−0.9538	−0.0341	1.0000	0.167
SGII	−2645.00	340.00	−41.90	15595.00	105.00	0.0900	−0.0588	1.4250	0.0604	1.0000	0.167
RAPT	−2160.00	513.00	121.00	11600.00	120.00	0.4180	−0.3600	−2.290	0.5860	1.0000	0.500
SV-bas	−1879.64	313.75	112.68	12527.38	124.63	0.2585	−0.3817	−2.8236	0.1232	0.5474	0.300
SV-m56-O	−1905.40	571.19	1594.80	8439.04	133.27	0.6440	−2.9737	−1.2553	1.7966	0.7949	0.200
SV-m64-O	−2083.86	484.60	1134.35	10720.67	113.97	0.6198	−2.3327	−1.3059	1.2101	1.1042	0.200
SV-min	−2112.25	295.78	142.27	13988.57	111.29	0.2439	−1.4349	−2.6259	0.2581	0.8255	0.255
T6	−1794.20	294.00	−294.00	12817.00	107.00	0.3920	−0.5000	−0.5000	0.5000	1.0000	0.333

The parameters are given in the units: t_0 (MeV fm^3), t_1 (MeV fm^5), t_2 (MeV fm^5), t_3 (MeV fm$^{3(\alpha+1)}$), W_0 (MeV fm^5).

Table 2. Symmetric NM properties at saturation density ρ_0(fm^3) associated with the 20 Skyrme-type interactions of table 1.

Force	ρ_0	$K_{\rm NM}$	m^*/m	κ
KDE0	0.161	228.8	0.72	0.30
KDE0v1	0.165	227.5	0.74	0.23
SLy4	0.160	229.9	0.70	0.25
SLy5	0.160	229.9	0.70	0.25
SLy6	0.159	229.8	0.69	0.25
SK255	0.157	225.0	0.80	0.54
SKI2	0.158	240.9	0.68	0.25
SKI3	0.158	258.1	0.58	0.25
SKI5	0.156	255.7	0.58	0.25
SKM*	0.160	216.7	0.79	0.53
SKMP	0.157	230.9	0.65	0.71
SKP	0.162	200.8	1.00	0.30
LNS	0.175	210.8	0.83	0.38
SGII	0.159	215.0	0.79	0.49
RAPT	0.160	239.51	0.67	0.78
SV-bas	0.160	234.0	0.90	0.40
SV-m56-O	0.157	254.6	0.56	0.60
SV-m64-O	0.159	241.4	0.64	0.60
SV-min	0.161	222.0	0.95	0.08
T6	0.161	235.93	1.00	0.00

Also the values of the incompressibility modulus $K_{\rm NM}$ (MeV), isoscalar effective mass m^*/m and the enhancement factor κ are given.

The NM EOS is important to understand many phenomena such as the collective excitation of nuclei. Giant resonances (GRs) are a highly collective behaviour of the atomic nuclei in which almost all the nucleons participate. In the microscopic picture, GRs can be described as a coherent superposition of particle–hole excitations. In random phase approximation (RPA), the collective excitation can be described as a linear combination of particle–hole configurations in both excited and ground states. The self-consistent Skyrme Hartree–Fock (HF)-based [15] RPA has been very successful in providing a microscopic description of phenomena associated with collective excitations in the nuclei [16,17]. To understand the structural and bulk properties of nuclear systems, the $S(E)$ peak of low-lying energies was studied for years based on the fully self-consistent HF-RPA with Skyrme-type interaction [18].

Having a large number of Skyrme-force parameterisations requires continuous search for the best to describe the experimental data. Here, in the framework of self-consistent HF-RPA with 20 Skyrme-type nucleon–nucleon effective interactions, we examine various collective modes, which are based on the experimental data on the $S(E)$ distribution of the isoscalar giant monopole resonance (ISGMR), $J^\pi = 0^+$, $T = 0$, the isovector giant dipole resonance (IVGDR), $J^\pi = 1^-$, $T = 1$ and isoscalar giant quadrupole resonance (ISGQR), $J^\pi = 2^+$, $T = 0$ of the ^{40}Ca and ^{48}Ca nuclei. Moreover, we discussed the sensitivity of the centroid energy m_1/m_0 and moment m_1 of the $S(E)$ to bulk properties of NM, such as $K_{\rm NM}$, the effective mass m^*/m and the enhancement factor κ.

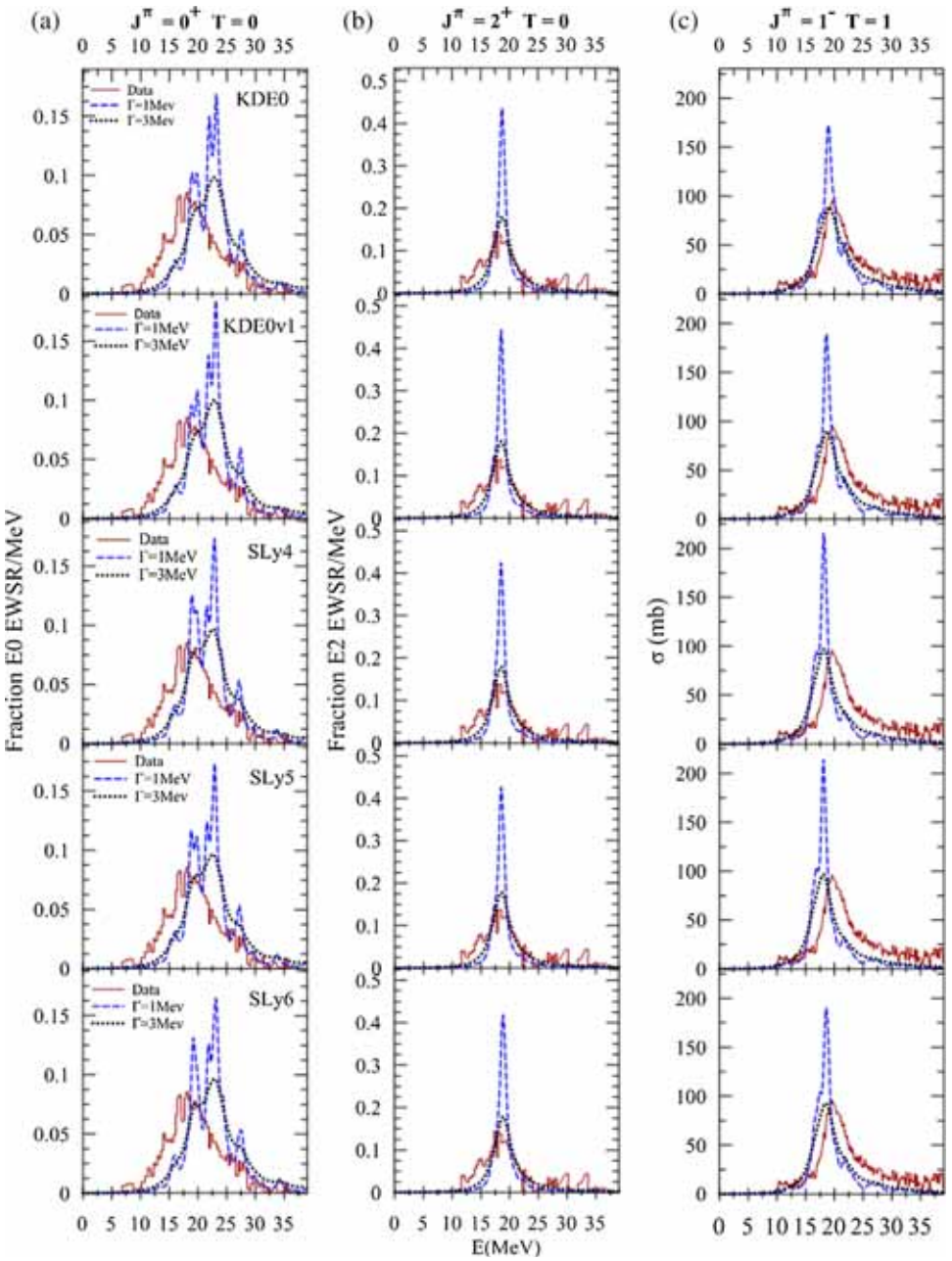

Figure 1. Self-consistent HF-based RPA results for the distribution of the fraction of EWSR for (**a**) isoscalar monopole ($E0$), (**b**) quadrupole ($E2$) and (**c**) photoabsorption dipole cross-section ($E1$) in ^{40}Ca, obtained using the KDE0, KDE0v1, SLy4, SLy5 and SLy6 Skyrme interactions. A Lorentzian smearing Γ of 1 MeV (blue dashed lines) and 3 MeV (black dotted lines) width was used in the calculation. Experimental data from ref. [33] for ISGMR and ISGQR and from [35] for IVGDR, are shown as red solid lines.

2. Formalism

The strength functions are defined by the transition operators as follows:

$$S(E) = \sum_{\nu} |\langle \nu | \hat{F}_J | 0 \rangle|^2 \delta(E - E_\nu), \tag{1}$$

following the fully self-consistent HF-RPA with Skyrme-type interaction [16,17], $|0\rangle$ is the RPA ground state and the sum is the overall RPA excitation state $|\nu\rangle$ with the corresponding excitation energy E_ν. The single-particle scattering operator $\hat{F}_J$ is given by

$$\hat{F}_J = \begin{cases} \sum_i f_J(r_i) Y_{J0}(i), & T=0, \\ \frac{Z}{A} \sum_n f_J(r_n) Y_{J0}(n) - \frac{N}{A} \sum_p f_J(r_p) Y_{J0}(p), & T=1, \end{cases} \tag{2}$$

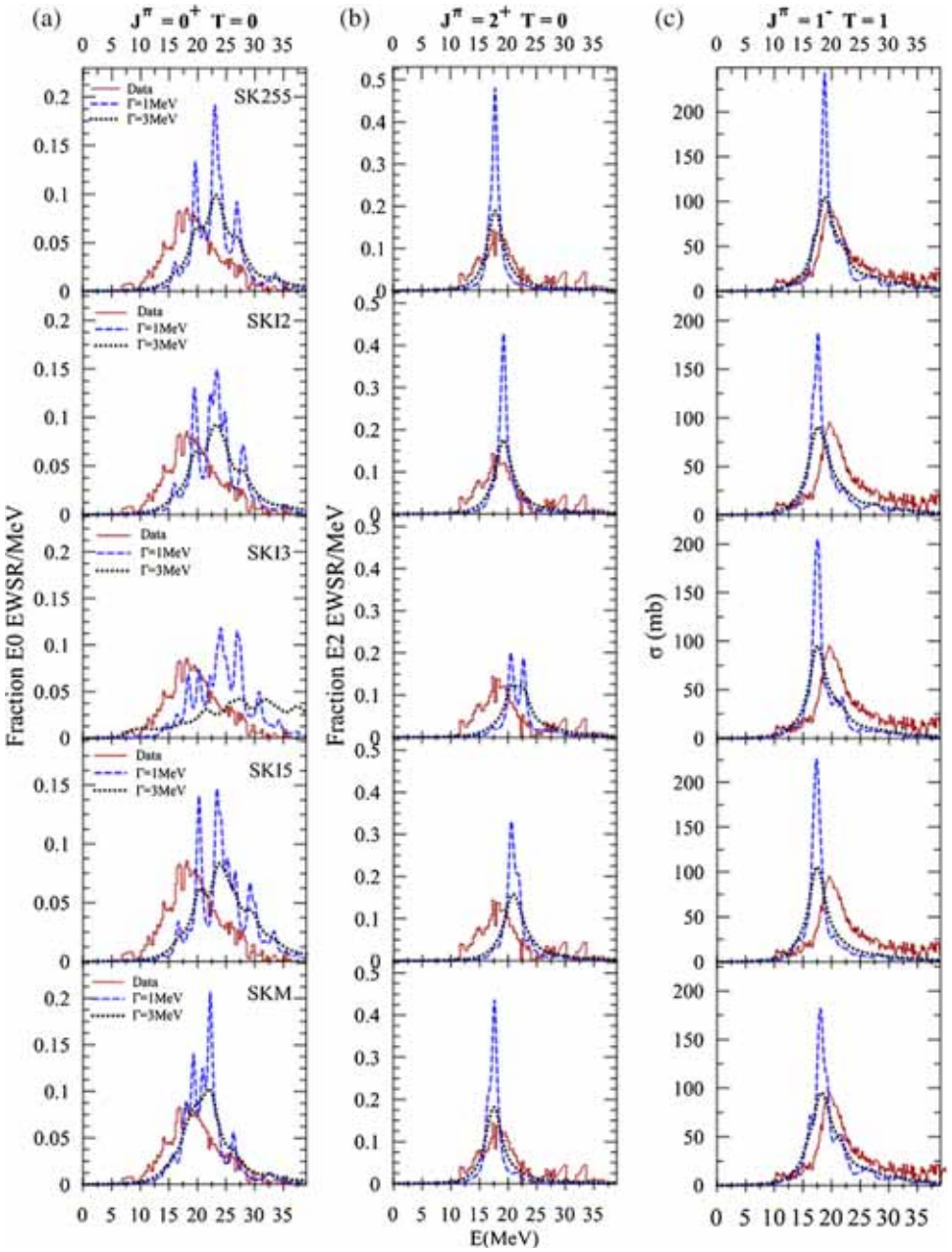

Figure 2. Same as figure 1 except that the results are obtained using for the SK255, SKI2, SKI3, SKI5 and SKM Skyrme interactions.

The function $f_J(r)$ is arbitrary and it often corresponds to the spherical Bessel function $j_J(qr)$ for electromagnetic external fields, where q is the photon momentum, or it becomes proportional to $r^J(i)$ in the long wavelength limit. For isovector dipole excitation $f(r) = r$, whereas for the isoscalar dipole $f(r) = r^3 - (5/3)\langle r^2\rangle r$ to avoid the undesired effect of the overlap between the spurious state and the physical states. For the isoscalar and isovector monopole, quadrupole excitations $f(r) = r^2$, r^2 and r^3, respectively.

The sum rule or energy moment is related to a strength function as follows:

$$m_k = \int E^k S(E)\,\mathrm{d}E \tag{3}$$

and it gives the kth moment of the excitation strength distribution produced by the operator $\hat{F}_J$.

The energy moment m_1 (energy-weighted sum rule, or EWSR) can also be calculated using the HF ground-state wave function. For the isoscalar operator $\hat{F}_J$, the EWSR is given by

$$m_1^{(\mathrm{IS})}(J) = \frac{\hbar^2}{2m}\frac{A}{4\pi}(2J+1)\,\langle g_J\rangle, \tag{4}$$

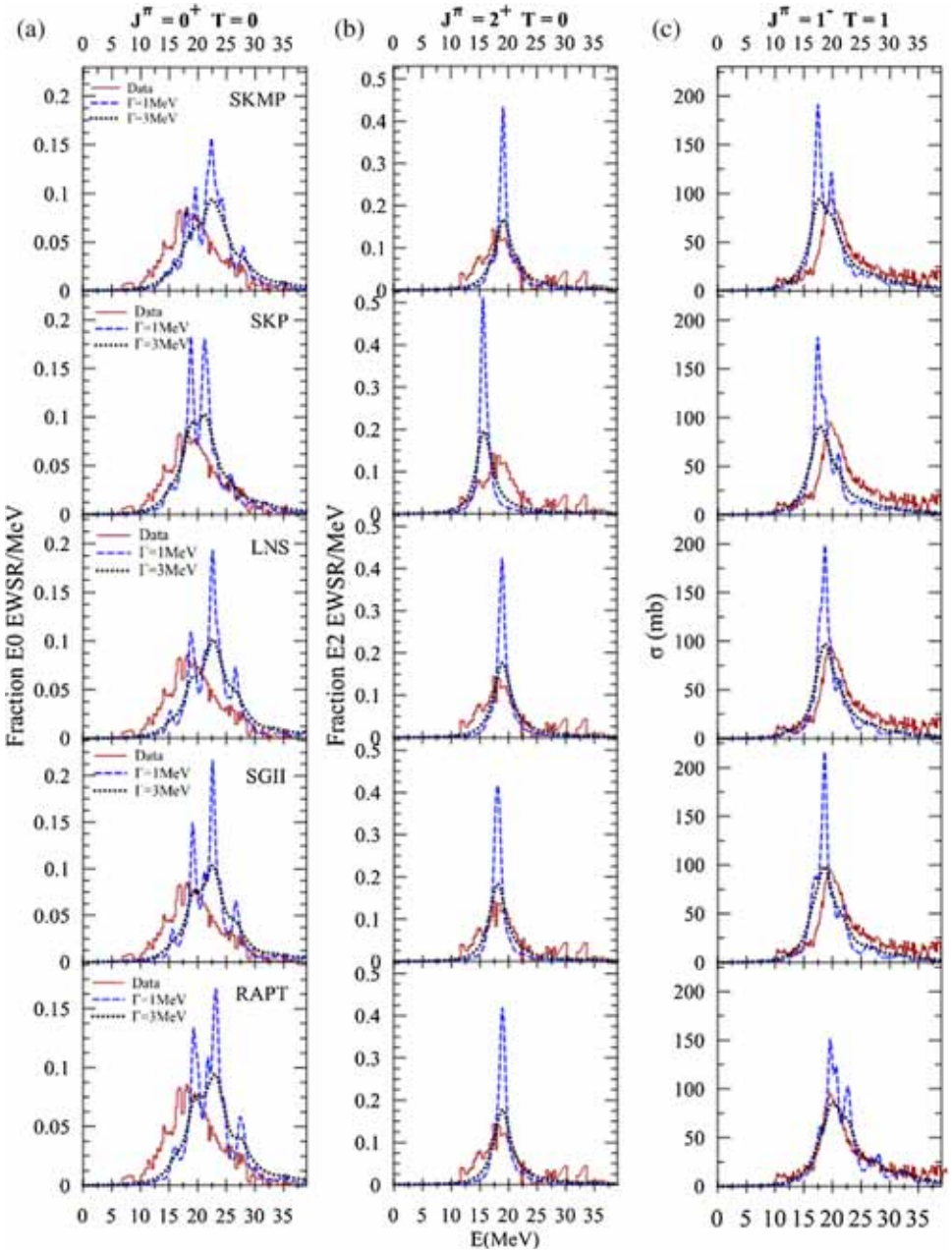

Figure 3. Same as figure 1 except that the results are obtained using the SKMP, SKP, LNS, SGII and RAPT Skyrme interactions.

where

$$\langle g_J \rangle = \frac{1}{A} \int g_J(r)\rho(r)\mathrm{d}^3r, \tag{5}$$

$$g_J(r) = \left(\frac{\mathrm{d}f_J}{\mathrm{d}r}\right)^2 + J(J+1)\left(\frac{f_J}{r}\right)^2, \tag{6}$$

where $\rho(r)$ is the HF ground-state matter density distribution. For the isovector operator $\hat{F}_J$, the velocity-dependent terms of the Skyrme interaction contribute to the enhancement factor κ and the EWSR is given by

$$m_1^{(\mathrm{IV})}(J) = m_1^{(\mathrm{IS})}(J)(1+\kappa), \tag{7}$$

where

$$\kappa = \frac{2m/\hbar^2}{A\langle g_J \rangle}\left(t_1\left(1+\frac{x_1}{2}\right) + t_2\left(1+\frac{x_2}{2}\right)\right) \times \int g_J(r)\rho_n(r)\rho_p(r)\mathrm{d}^3r, \tag{8}$$

where t_1 and x_1 are the parameters of the Skyrme interaction.

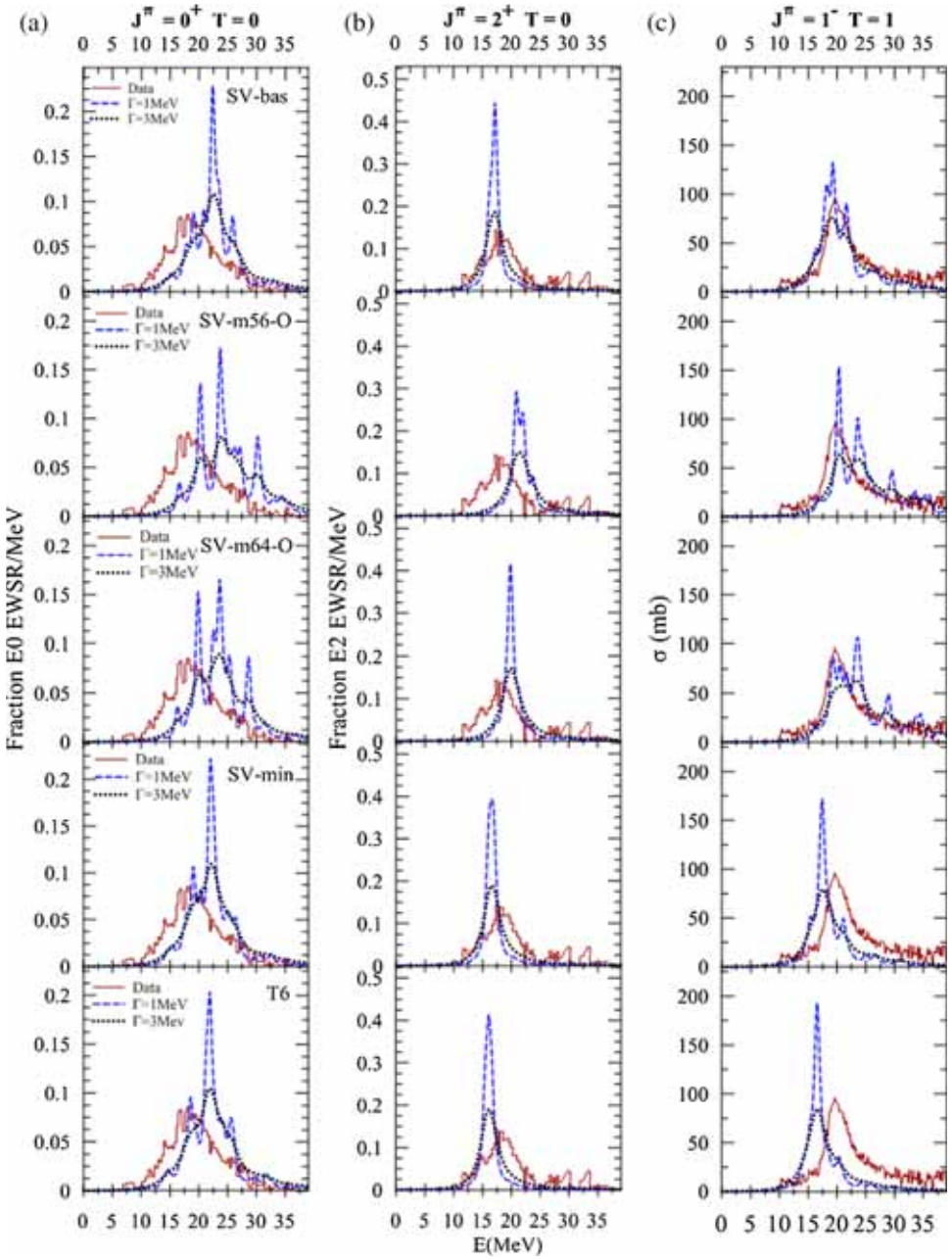

Figure 4. Same as figure 1 except that the results are obtained using the SV-bas, SV-m56-O, SV-m64-O, SV-min and T6 Skyrme interactions.

The centroid can be computed as follows:

$$E_{\mathrm{CEN}} = \frac{m_1}{m_0}. \tag{9}$$

For plotting, the strength function is approximated as follows:

$$S(E) = \sum_{\nu} |\langle \nu \| \hat{F}_J \| 0 \rangle|^2 \rho_\Gamma (E - E_\nu), \tag{10}$$

where the Lorentzian function is defined as follows:

$$\rho_\Gamma (E - E_\nu) = \frac{\Gamma}{2\pi} \frac{1}{(E - E_\nu)^2 + (\Gamma/2)^2} \tag{11}$$

with Γ being the smearing parameter.

3. Results and discussion

Here, we present the results of the fully self-consistent HF-dependent RPA matrix of the strength functions and

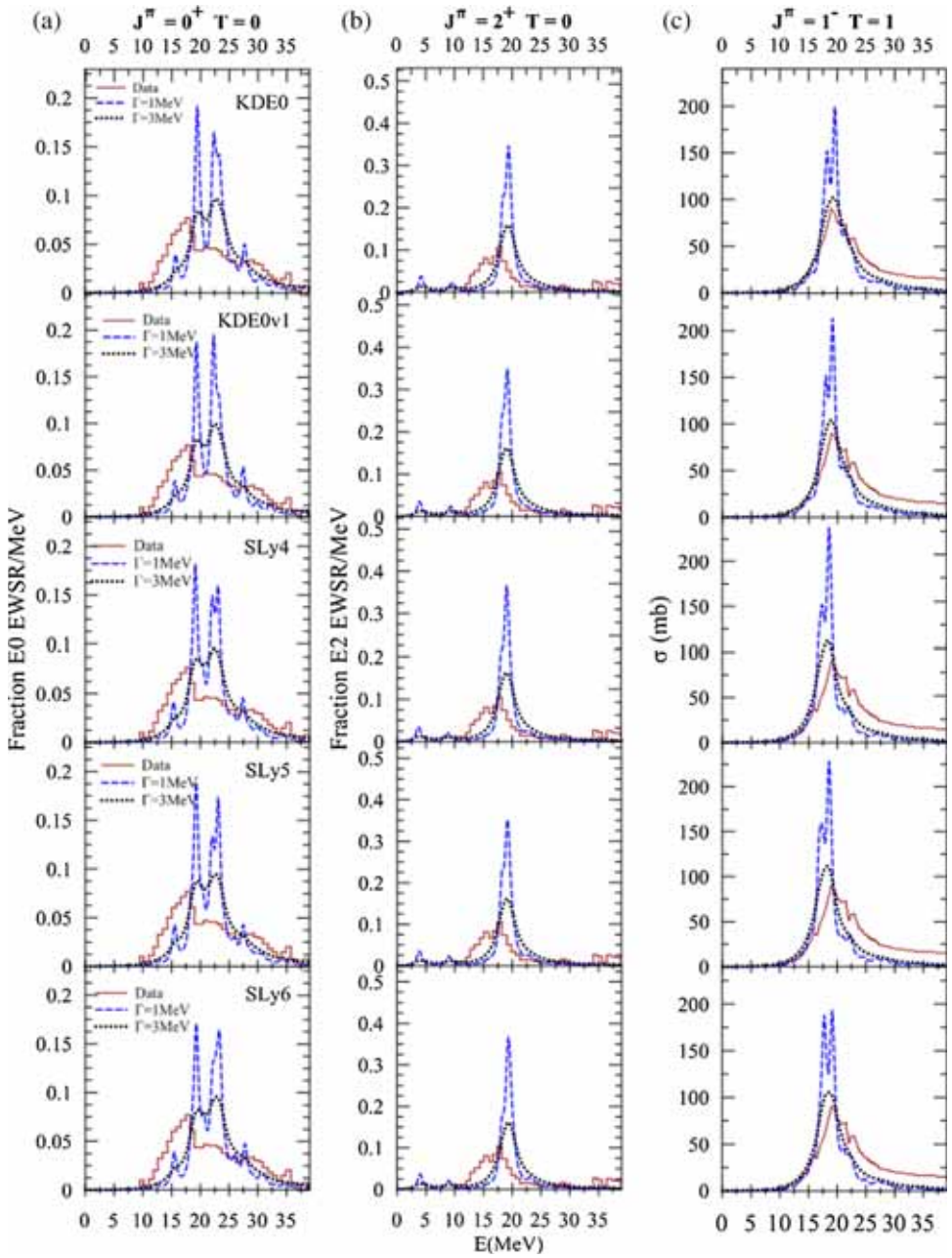

Figure 5. Self-consistent HF-based RPA results for the distribution of the fraction of EWSR for (**a**) isoscalar monopole ($E0$), (**b**) quadrupole ($E2$) and (**c**) photoabsorption dipole cross-section ($E1$) in ^{48}Ca, obtained using the KDE0, KDE0v1, SLy4, SLy5 and SLy6 Skyrme interactions. A Lorenzian smearing Γ of 1 MeV (blue dashed lines) and 3 MeV (black-dotted lines) width was used in the calculation. Experimental data from ref. [34] for ISGMR and ISGQR and from [35] for IVGDR, are shown as red solid lines.

centroid energies. Strength function calculations have been done in the long wavelength limit. The three-dimensional HF equations of ref. [16] are simplified into a set of radial one-dimensional differential equations. The radial HF equations are solved numerically by using Numerov's formula [18]

$$y_{i+1} = \frac{(12 - 10\,f_n)y_i - f_{n-1}y_{i-1}}{f_{n+1}}, \tag{12}$$

and the auxiliary array f_n is defined as

$$f_n \equiv 1 + g_n \frac{(\Delta x)^2}{12},$$

where

$$g_n = \frac{2m}{\hbar^2}[E - V]. \tag{13}$$

We concentrate on the three most important aspects of GR: the ISGMR, $J^\pi = 0^+$, $T = 0$, the IVGDR,

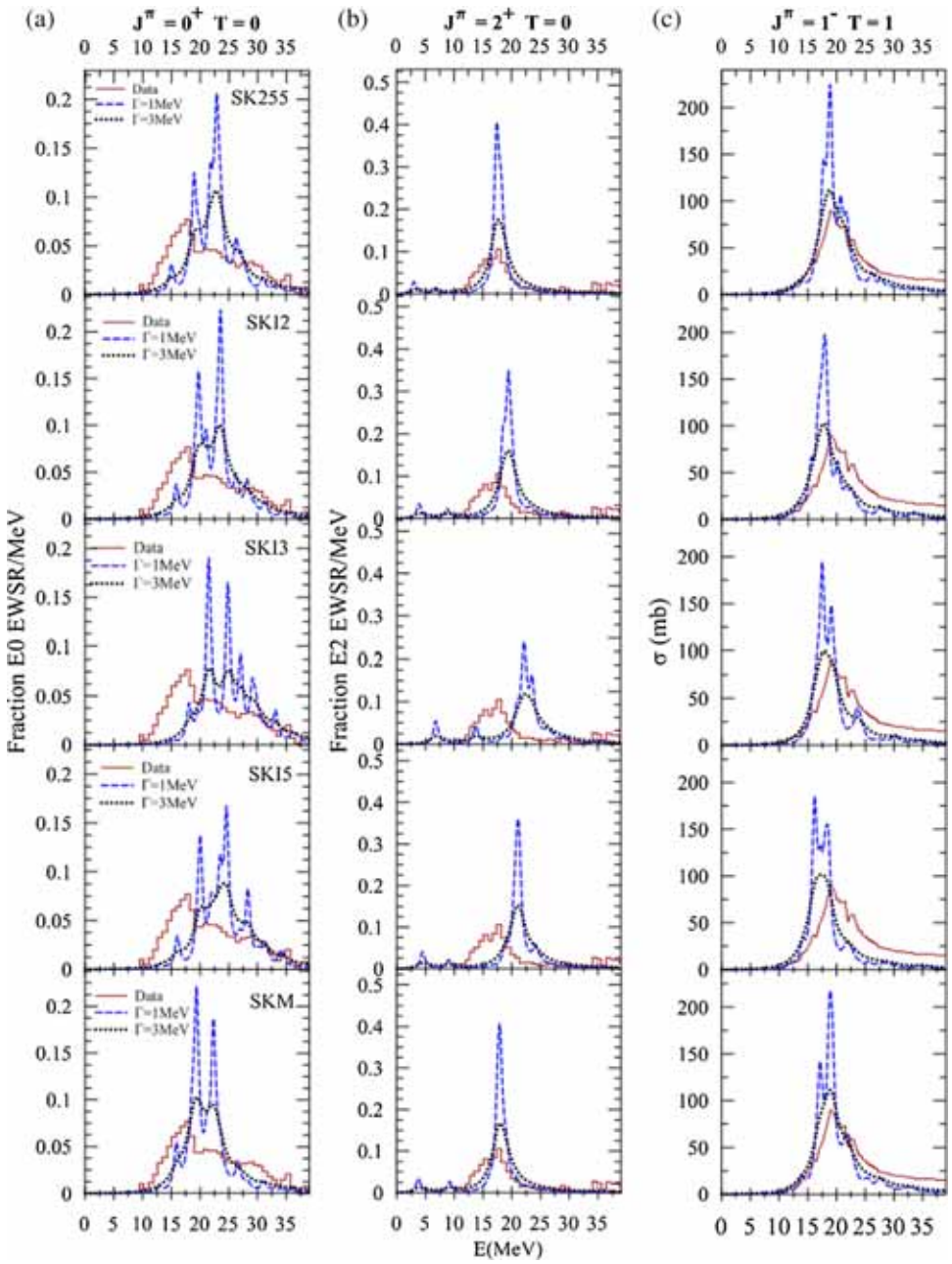

Figure 6. Same as figure 5 except that the results are obtained using the SK255, SKI2, SKI3, SKI5 and SKM Skyrme interaction.

$J^\pi = 1^-$, $T = 1$ and ISGQR, $J^\pi = 2^+$, $T = 0$ in ^{40}Ca and ^{48}Ca nuclei. Twenty Skyrme-type interactions, KDE0 [19], KDE0v1 [20], SLy4 [21], SLy5 [22], SLy6 [22], SK255 [22], SKI2 [23], SKI3 [23], SKI5 [23], SKM [24], SKMP [25], SKP [26], LNS [27], SGII [28], RAPT [29], SV-bas [30], SV-m56-O [31], SV-m64-O [31], SV-min [32] and T6 [32], shown in table 1 were investigated. The RPA matrix diagonalisation was performed within the model space and all the particle–hole configurations were included. The interactions are associated with the ranges of NM properties in table 2: $K_{\rm NM} = 201-258$ MeV, $m^*/m = 0.56-1.00$ and $\kappa = 0.08-0.71$.

The strength distributions (fraction of EWSR) of isoscalar monopole $E0$, quadrupole $E2$ and isovector dipole $E1$ photoabsorption cross-sections (mb) are shown in figures 1–8 for the investigated nuclei ^{40}Ca and ^{48}Ca, respectively. Lorentzian smearing Γ of 1 and 3 MeV width was used in the calculation and compared with the experimental data [33,34]. Most of the interactions agree with the experimental data, especially with $\Gamma = 3$ MeV. Close to 100% of isoscalar

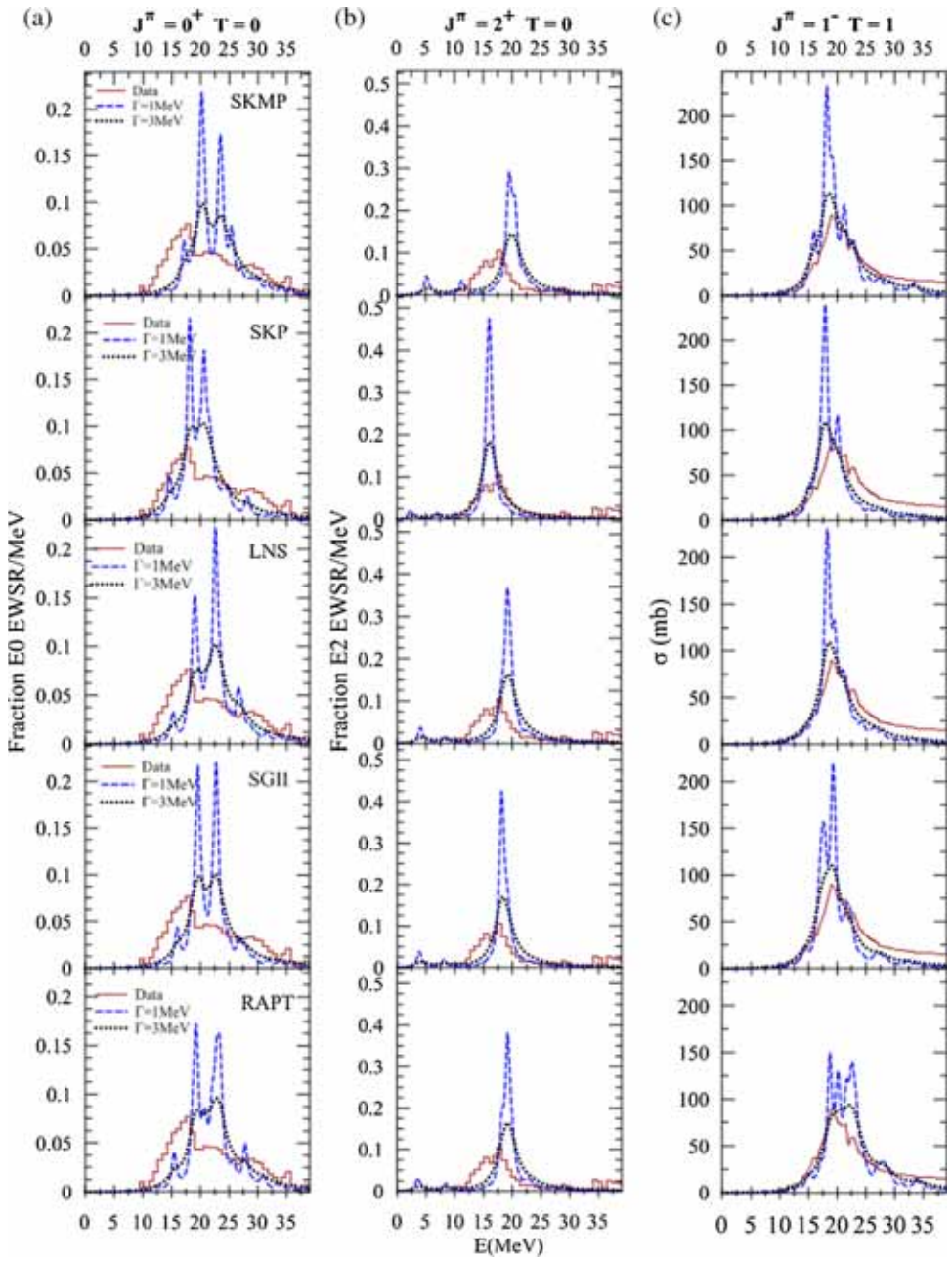

Figure 7. Same as figure 5 except that the results are obtained using the SKMP, SKP, LNS, SGII and RAPT Skyrme interactions.

$E0$ and $E2$ strength were located between 9.5 and 40 MeV and isovector $E1$ between 0 and 40 MeV. SkM interaction works best and agrees with data concerning peak hight, widths and (smooth) profiles of strength. For ISGMR, a fragmented structure was seen in some interactions.

The peak energy is defined as the centroid energy m_1/m_0, where the moment m_1 was taken in a certain energy interval around the resonance peak. Theoretical results of m_1/m_0 (MeV) and m_1 (%EWSR) for ISGMR, ISGQR and IVGDR in ^{40}Ca and ^{48}Ca are presented in table 3 and compared with the experimental data. We use the excitation energy range of 9.5–40 MeV for ISGMR and ISGQR and the range of 0–40 MeV for IVGDR.

m_1/m_0 is related to $K_{\rm NM}$. High $K_{\rm NM}$ shifts the peak to upper energy while low $K_{\rm NM}$ shifts the peak to lower energy, like SKI3 interaction with $K_{\rm NM} = 258.1$ MeV results in the centroid energy equal to 24.96 and 24.38 in ^{40}Ca and ^{48}Ca, respectively, while the experimental value of $m_1/m_0 = 19.18 \pm 0.37$ MeV for ^{40}Ca and $m_1/m_0 = 19.88 \pm 0.16$ MeV for ^{48}Ca [34]. The

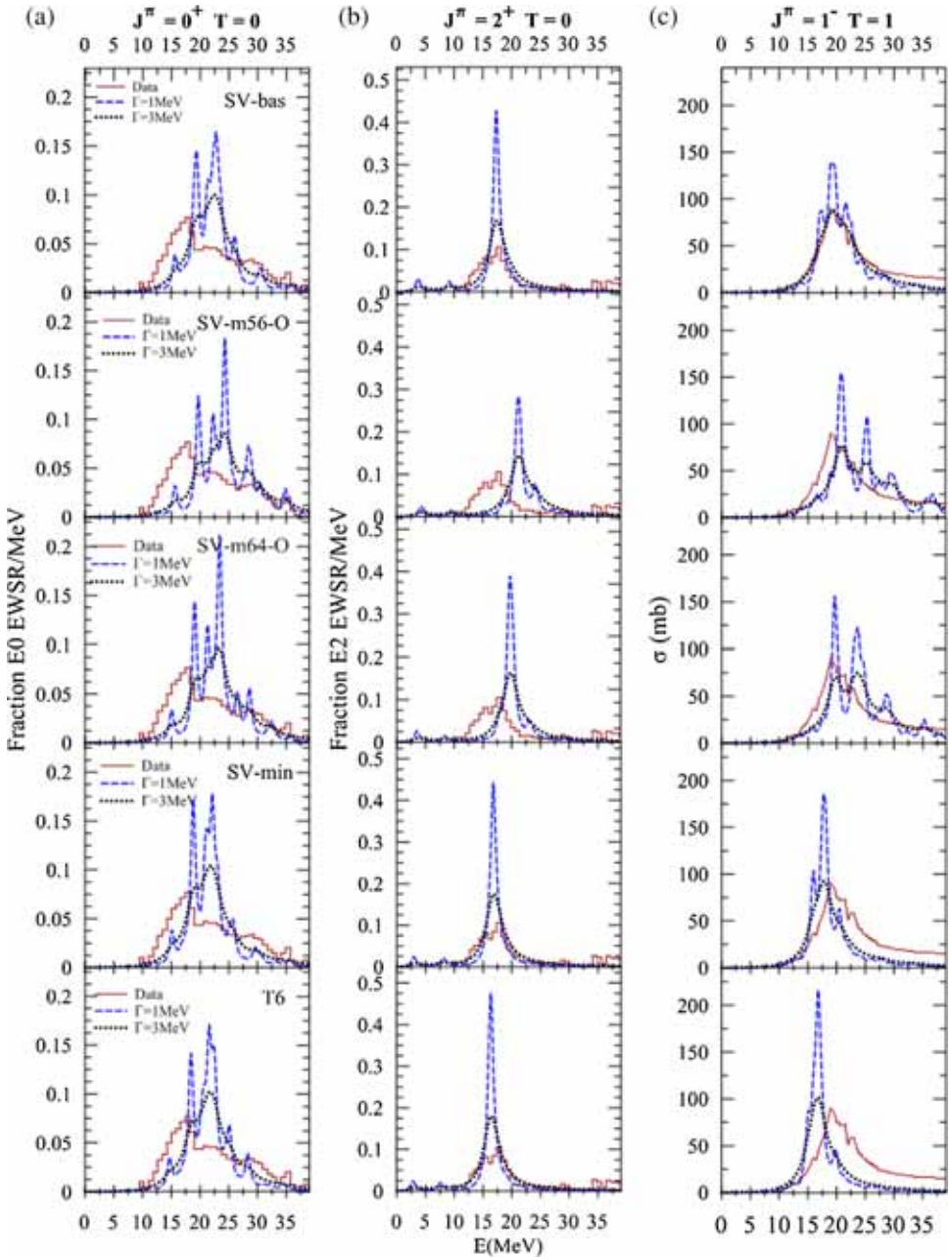

Figure 8. Same as figure 5 except that the results are obtained using the SV-bas, SV-m56-O, SV-m64-O, SV-min and T6 Skyrme interactions.

interactions (SKM* and SKP) with $K_{\rm NM}$ = (216.7 and 200.8 MeV), respectively, produce ISGMR at the same energy but with simple difference in moment m_1.

For ISGMR, m_1/m_0 values of ^{40}Ca are higher than the experimental values, but in ^{48}Ca, they are more consistent with the experimental values similar to the SKP interaction which has the same energy as the experimental value (≈19.88 MeV), while the experimental data show that ISGMR in ^{40}Ca lies at a lower energy than in ^{48}Ca. Nineteen of the Skyrme interactions of table 3 show ISGMR in ^{40}Ca at a higher energy than in ^{48}Ca, except the SKMP interaction at a higher energy in ^{48}Ca than in ^{40}Ca.

The interactions SK255, SKM and SV-bas having $m^*/m = 0.80$, 0.79 and 0.90, respectively, in ^{40}Ca and interaction SKI3 with $m^*/m = 0.58$ in ^{48}Ca, reproduce m_1/m_0 experimental data for ISGQR ($m_1/m_0 = 17.84 \pm 0.43$ MeV for ^{40}Ca [33] and $m_1/m_0 = 18.61 \pm 0.24$ MeV of ^{48}Ca [34]). m_1/m_0 values of IVGDR of ^{40,48}Ca were close to the experimental values with the enhancement factor κ in the range 0.2–0.6, but we did not notice any dependence of m_1 on $K_{\rm NM}$, m^*/m and κ.

Table 3. Theoretical results of m_1/m_0 (MeV) and m_1 (%EWSR) for ISGMR, ISGQR and IVGDR in ^{40}Ca and ^{48}Ca are compared with the experimental data.

	ISGMR				ISGQR				IVGDR			
	^{40}Ca		^{48}Ca		^{40}Ca		^{48}Ca		^{40}Ca		^{48}Ca	
	m_1/m_0	m_1	m_1/m_0	m_1	m_1/m_0	m_1	m_1/m_0	m_1	m_1/m_0	m_1	m_1/m_0	m_1
Experiment	19.18 ± 0.37	97 ± 11	19.88 ± 0.16	95^{+11}_{-15}	17.84 ± 0.43	108 ± 12	18.61 ± 0.24	83^{+10}_{-16}	19.8 ± 0.5		19.5 ± 0.5	
KDE0	21.85	92.53	21.74	92.83	18.77	96.70	15.42	97.68	19.46	99.59	19.58	99.51
KDE0v1	21.76	92.82	21.58	92.91	18.58	96.74	15.26	97.64	19.07	99.71	19.17	99.62
SLy4	21.40	93.10	21.23	93.47	18.53	97.19	15.04	97.85	18.37	99.75	18.38	99.68
SLy5	21.41	93.06	21.30	93.42	18.56	97.13	15.12	97.88	18.24	99.74	18.29	99.67
SLy6	21.78	92.36	21.59	92.98	18.87	96.85	15.29	97.64	18.76	99.73	18.75	99.65
SK255	22.71	94.99	21.89	93.96	17.80	97.86	14.22	98.14	19.70	99.64	19.65	99.65
SKI2	22.57	91.19	22.05	92.47	19.33	96.33	15.55	97.60	18.39	99.68	18.31	99.63
SKI3	24.96	68.55	24.38	89.78	21.67	94.74	18.36	96.63	18.23	99.64	18.78	99.48
SKI5	23.75	89.46	23.29	89.85	21.11	96.27	16.59	96.96	17.79	99.96	17.66	99.93
SKM	20.77	95.65	20.62	94.45	17.50	97.79	14.56	98.33	18.96	99.52	19.30	99.52
SKMP	21.63	92.30	21.92	91.89	19.28	96.68	16.16	98.00	19.10	98.60	19.71	98.68
SKP	20.30	98.88	19.61	98.69	15.76	99.08	13.11	99.10	18.56	99.95	18.67	99.91
LNS	21.89	90.57	21.59	91.31	18.95	95.53	15.36	96.76	19.29	99.50	19.39	99.39
SGII	21.56	92.58	21.21	93.34	18.11	96.91	14.65	97.94	19.14	99.52	19.22	99.53
RAPT	21.88	92.78	21.47	93.24	18.97	97.05	15.39	97.91	21.35	99.80	21.49	98.98
SV-bas	21.87	96.54	21.61	94.23	17.08	97.65	14.4	98.27	20.05	99.75	20.34	99.67
SV-m56-O	24.09	89.03	23.51	89.44	21.74	95.42	17.84	95.65	23.72	98.41	23.39	98.47
SV-m64-O	22.91	90.61	22.14	92.21	20.05	95.98	16.25	97.07	23.22	98.84	22.93	98.90
SV-min	21.43	97.11	20.94	94.77	16.58	98.07	13.92	98.36	18.22	99.76	18.25	99.67
T6	21.36	97.42	20.93	98.14	16.08	98.32	13.47	98.77	16.94	99.75	16.98	99.65

4. Conclusions

In summary, we have carried out our fully self-consistent HF-based RPA calculation for the strength function of ISGMR (0^+, 0), IVGDR (1^-, 1) and ISGQR (2^+, 0). Close to 100% of isoscalar $E0$ and $E2$ strength have been located between 9.5 and 40 MeV and isovector $E1$ between 0 and 40 MeV for both ^{40}Ca and ^{48}Ca. For each resonance, the energy centroids are computed as the ratio m_1/m_0 where the moments m_1 are taken in a certain energy interval around the resonance peak. The energy centroid of ISGMR in ^{48}Ca is higher than those of ^{40}Ca, but self-consistent microscopic calculation with 19 Skyrme interaction predict lower centroid energies for ^{48}Ca compared to ^{40}Ca.

It is important to carry out fully self-consistent HF-RPA calculations to extract an accurate value of $K_{\rm NM}$ from the experimental data on ISGMR. Therefore, we had presented the correlation between the energy centroid and the coefficient $K_{\rm NM}$. The conclusion can be drawn that $K = 240 \pm 20$ MeV. The uncertainty of about 20 MeV is mainly due to the uncertainty in the value of the overall shape of the NM symmetry energy curve, as a function of density.

We have found that an agreement with the experimental data of m_1/m_0 of ISGQR in ^{40,48}Ca is obtained for the value of the effective mass in the range of $m^*/m = 0.5-1$. For ISGMR, m_1/m_0 is increasing with $K_{\rm NM}$, but m_1 is approximately constant. m_1/m_0 of IVGDR of ^{40,48}Ca is close to the experimental results with the enhancement factor κ in the range 0.2–0.6, but we did not notice any dependence of m_1 on $K_{\rm NM}$, m^*/m and κ.

References

[1] S C Pieper and R B Wiringa, *Annu. Rev. Nucl. Part. Sci.* **51**, 53 (2001)
[2] B R Barrett, P Navrátil and J P Vary, *Prog. Part. Nucl. Phys.* **69**, 131 (2013)
[3] G Hagen, T Papenbrock, M Hjorth-Jensen and D J Dean, *Rep. Prog. Phys.* **77**(**9**), 096302 (2014)
[4] A Cipollone, C Barbieri and P Navrátil, *Phys. Rev. Lett.* **111**(**6**), 062501 (2013)
[5] H Hergert, S Binder, A Calci, J Langhammer and R Roth, *Phys. Rev. Lett.* **110**(**24**), 242501 (2013)
[6] G Colò, *Phys. Part. Nucl.* **39**(**2**), 286 (2011)
[7] A Bohr and B M Mottelson, *Nuclear structure II* (Benjamin, New York, 1975)
[8] P Ring and P Schuck, *The nuclear many-body problem* (Springer, New York, 1980)
[9] S Shlomo, V M Kolomietz and G Colo, *Eur. Phys. J. A* **30**, 23 (2006), and references therein
[10] N K Glendenning, *Phys. Rev. C* **37**, 2733 (1988)
[11] W D Myers and W J Swiatecki, *Phys. Rev. C* **57**, 3020 (1998)
[12] L Satpathy, V S U Maheshwari and R C Nayak, *Phys. Rep.* **319**, 85 (1999)
[13] S Shlomo, T Sil, V Kim Au and O G Pochivalov, *Phys. Atom. Nucl.* **69**(**7**), 1132 (2006)
[14] M R Anders, S Shlomo, T Sil, D H Youngblood and Y-W Lui and Fnu Krishichayan, *Phys. Rev. C* **87**, 024303 (2013)
[15] A N Abdulla, *Pramana – J. Phys.* **89**(**3**): 42 (2017)
[16] G Colò, L Cao, N Van Giai and L Capelli, *Comput. Phys. Commun.* **184**, 142 (2013)
[17] Ali H Taqi and M S Ali, *Indian J. Phys.* **92**(**1**), 69 (2017)
[18] P Giannozzi, *Numerical methods in quantum mechanics*, Lecture notes, https://archive.org/details/Paolo_Giannozzi_Numerical_Methods_in_Quantum_Mechanics (University of Udine, 2018)
[19] M N Harakeh and A M van der Woude, *Giant resonances: Fundamental high-frequency modes of nuclear excitations* (Oxford University Press, London, 2001)
[20] B K Agrawal, S Shlomo and V K Au, *Phys. Rev. C* **72**, 014310 (2005)
[21] E Chabanat, P Bonche, P Haensel, J Meyer and R Schaeffer, *Nucl. Phys. A* **635**, 231 (1998)
[22] B K Agrawal, S Shlomo and V Kim Au, *Phys. Rev. C* **68**, 031304 (2003)
[23] P-G Reinhard and H Flocard, *Nucl. Phys. A* **587**, 467 (1995)
[24] J Bartel, P Quentin, M Brack, C Guet and H B Hakansson, *Nucl. Phys. A* **386**, 79 (1982)
[25] L Bennour, P-H Heenen, P Bonche, J Dobaczewski and H Flocard, *Phys. Rev. C* **40**, 2834 (1989)
[26] J Dobaczewski, H Flocard and J Treiner, *Nucl. Phys. A* **422**, 103 (1984)
[27] L G Cao, U Lombardo, C W Shen and N V Giai, *Phys. Rev. C* **73**, 014313 (2006)
[28] N Van Giai and H Sagawa, *Phys. Lett. B* **106**, 379 (1981)
[29] M Rayet, M Arnould, F Tondeur and G Paulus, *Astron. Astrophys.* **116**, 183 (1982)
[30] P Klupfel, P-G Reinhard, T J Burvenich and J A Maruhn, *Phys. Rev. C* **79**, 034310 (2009)
[31] N Lyutorovich, V I Tselyaev, J Speth, S Krewald, F Grummer and P-G Reinhard, *Phys. Rev. Lett.* **109**, 092502 (2012)
[32] F Tondeur, M Brack, M Farine and J M Pearson, *Nucl. Phys. A* **420**, 297 (1984)
[33] D H Youngblood, Y-W Lui and H L Clark, *Phys. Rev. C* **63**, 067301 (2001)
[34] Y-W Lui, D H Youngblood, S Shlomo, X Chen, Y Tokimoto, Fnu Krishichayan, M Anders and J Button, *Phys. Rev. C* **83**, 044327 (2011)
[35] V A Erokhova, M A Yolkin, A V Izotova, B S Ishkhanov, I M Kapitonov, E I Lileeva and E V Shirokov, *Izv. Ross. Akad. Nauk, Ser. Fiz.* **67**, 1479 (2003) [*Bull. Russ. Acad. Sci. Phys.* **67**, 1636 (2003)]